Frontiers in Health Informatics
ISSN-Online: 2676-7104
www.healthinformaticsjournal.com
2024; Vol 13: Issue 8
Open Access

Morphology and Band Gap Controlled Studies of CdS_xSe_{1-x} Films Deposited by Laser Ablation

Priti Singh* and Neeraj Jaiswal

Department of Chemistry, K.S. Saket P.G. College, Ayodhya, India

Cite this paper as: Priti Singh and Neeraj Jaiswal (2024) Morphology and Band Gap Controlled Studies of CdS_xSe_{1-x} Films Deposited by Laser Ablation. *Frontiers in Health Informatics, 13(8), 5818-5826*

Abstract

Through the utilization of the pulsed laser ablation technique, binary and ternary CdS_xSe_{1-x} films, with a value of $0 \leq x \leq 1$, were deposited on a quartz substrate. The formation of these films was accomplished by employing a pulsed Nd:YAG laser, maintaining a pressure of 4×10^{-6} Torr within the growth chamber, and maintaining a substrate temperature of 550 ºC. The hexagonal structure of the CdS_xSe_{1-x} semiconducting films was validated by XRD, which indicated that the films possessed a preferential orientation in the (002) plane. This orientation was associated with the films' exceptional crystal quality. The energy band gap (E_g) can be estimated with the help of transmittance spectra. The values that we have calculated for the ternaries are 1.78, 1.9, and 2.06 eV, whereas the values for CdSe are 1.68 eV and the values for CdS are 2.39 eV. All of the samples exhibited a robust luminescence emission when the temperature was at room temperature. Furthermore, Raman spectroscopy revealed that the phonons associated with LO-CdS and LO-CdSe were seen simultaneously in the compound of ternaries. There is a correlation between the content of sulfur and the changing intensities and positions of these peaks.

Key words: CdS_xSe_{1-x}, Laser ablation, UV-Vis Spectroscopy, Photoluminescence, Raman spectroscopy.

Introduction:

Numerous binary and ternary semiconductor compounds, such as the II-VI compounds, are presently being studied due to their exceptional optical and electrical characteristics. Binary compounds CdS and CdSe exhibit a stable wurtzite structure and possess a straight band gap[1-5]. Ternary compounds possess the characteristic that the energy band gap is adjustable; specifically, for CdS_xSe_{1-x}, this range varies from 1.72 to 2.42 eV by altering the concentrations of sulfur (S) and selenium (Se). The ternary CdS_xSe_{1-x} compounds are significant for the fabrication of photovoltaic and optoelectronic devices due to their great sensitivity in the near- infrared and visible spectra. The CdS_xSe_{1-x} semiconductor compounds have excellent photoconductive and photoluminescent capabilities, enabling their successful integration into a variety of devices, including diodes, photosensors, LEDs, and photoresistors.

Laser ablation technique has been consolidated as a good alternative for the deposition of semiconductor films due to the quality of the films that are produced as a result of having the ability to tailor some of their physical properties[6-8]. Although there are several techniques that have been used to process CdSxSe1-x thin films, laser ablation technique has been consolidated as a reliable alternative. The laser ablation technique makes use of a pulsed laser beam with a high energy density that is focused on the surface of the target in order to evaporate and generate a plasma that will condense on the substrate in order to form the film[9].

Material and Methods:

For the purpose of this study, a laser ablation technique was utilized to process a total of five samples of CdS_xSe_{1-x}. For the purpose of the laser ablation procedure, which was carried out at a pressure of 4 x 10^{-6} Torr, a turbomolecular pump was utilized in order to evacuate the vacuum chamber. The ablation procedure was carried out with the assistance of a Nd-YAG laser that had a pulse duration of 12 nsec, a repetition rate of 30 hertz, and a wavelength of 1064 nanometers. All of the samples were subjected to a laser beam with a power of mJ per pulse. An object consisting of crushed powder was the target of the laser beam's concentration. Five circular targets made of CdS, CdSe, $CdS_{0.75}Se_{0.25}$, $CdS_{0.5}Se_{0.5}$ and $CdS_{0.25}Se_{0.75}$ were utilized. Each target had a diameter of one inch and a thickness of 3 mm.

Compressing CdS and CdSe high purity powders (Aldrich 99.99 %) yielded the CdS and CdSe targets, whereas combining CdS and CdSe powders yielded the ternary compound targets. The following amounts were blended for the first target: CdS (6.94 g) and CdSe (3.06 g), for the second target: CdS (4.3 g) and CdSe (5.7 g), and for the third target: CdS (2.01 g) and CdSe (7.99 g). This was done since each target was constructed with 10 g of powder and the densities of the compounds were taken into account. A pressure of 1 kbar was used to obtain all targets. The ablated material was deposited on substrates that were 3 cm away from the intended surface. The ablated material was deposited on substrates that were three centimeters away from the intended surface. All through the ablation process, the substrate—fused quartz—was maintained at a temperature of 500 °C. Thirty minutes was the designated deposition time. To examine the samples' crystalline structure, X-ray diffraction was carried out in a θ - 2θ setup utilizing the Kα line of cooper (λ = 1.54 Å) in a Bruker Advance diffractometer. A Perkin Elmer Lambda 35 spectrometer was used in the twin beam setup to generate UV-Vis transmittance spectra. This allowed for the calculation of the energy band gap of the materials. Using the 442 nm line of a He-Cd laser to excite the photoluminescence and a He-Ne laser (633 nm) for the Raman, the photoluminescence and Raman spectra were recorded using the LabRam HR Evolution spectrometer. The optical microscope's 100X objective lens focused the laser beam on the sample, which deposited an intensity of about 30 mJ onto the film's surface.

Results:

In the case of the binary compounds CdSe and CdS films, the diffraction spectra reveal a main peak at $2\theta = 25.4°$ and $2\theta = 25.35°$, respectively (Fig. 1), which are associated with the (002) crystalline plane of the hexagonal phase[7]. In addition, the ternary compounds' main peaks can be seen between these two peaks. As the temperature rises, the nuclei orientation tends to develop perpendicular arrangements along the substrate, allowing the atoms to gain enough energy for nucleation. This results in the hexagonal phase, which is often most noticeable in CdS (II-VI) films formed at high temperatures. The deposit's orientation along the *c*-axis perpendicular to the substrate is explained by the occurrence of the (002) peak, which is associated with the hexagonal structure[10].

According to Bragg's Law[11], the interplanar distance *d* was determined by utilizing the location of the primary peak in each diffractogram.

$$d = \frac{n\lambda}{2\sin\theta} \quad (1)$$

with λ = 1.54 Å the wavelength of Kα copper emission, *n* any integer and θ the Bragg angle of reflection. According to previous report[12], the structural characteristics can also be connected to the interplanar distance *d*.

Material and Methods:

For the purpose of this study, a laser ablation technique was utilized to process a total of five samples of CdS_xSe_{1-x}. For the purpose of the laser ablation procedure, which was carried out at a pressure of 4 x 10^{-6} Torr, a turbomolecular pump was utilized in order to evacuate the vacuum chamber. The ablation procedure was carried out with the assistance of a Nd-YAG laser that had a pulse duration of 12 nsec, a repetition rate of 30 hertz, and a wavelength of 1064 nanometers. All of the samples were subjected to a laser beam with a power of mJ per pulse. An object consisting of crushed powder was the target of the laser beam's concentration. Five circular targets made of CdS, CdSe, $CdS_{0.75}Se_{0.25}$, $CdS_{0.5}Se_{0.5}$ and $CdS_{0.25}Se_{0.75}$ were utilized. Each target had a diameter of one inch and a thickness of 3 mm.

Compressing CdS and CdSe high purity powders (Aldrich 99.99 %) yielded the CdS and CdSe targets, whereas combining CdS and CdSe powders yielded the ternary compound targets. The following amounts were blended for the first target: CdS (6.94 g) and CdSe (3.06 g), for the second target: CdS (4.3 g) and CdSe (5.7 g), and for the third target: CdS (2.01 g) and CdSe (7.99 g). This was done since each target was constructed with 10 g of powder and the densities of the compounds were taken into account. A pressure of 1 kbar was used to obtain all targets. The ablated material was deposited on substrates that were 3 cm away from the intended surface. The ablated material was deposited on substrates that were three centimeters away from the intended surface. All through the ablation process, the substrate—fused quartz—was maintained at a temperature of 500 °C. Thirty minutes was the designated deposition time. To examine the samples' crystalline structure, X-ray diffraction was carried out in a θ - 2θ setup utilizing the Kα line of cooper (λ = 1.54 Å) in a Bruker Advance diffractometer. A Perkin Elmer Lambda 35 spectrometer was used in the twin beam setup to generate UV-Vis transmittance spectra. This allowed for the calculation of the energy band gap of the materials. Using the 442 nm line of a He-Cd laser to excite the photoluminescence and a He-Ne laser (633 nm) for the Raman, the photoluminescence and Raman spectra were recorded using the LabRam HR Evolution spectrometer. The optical microscope's 100X objective lens focused the laser beam on the sample, which deposited an intensity of about 30 mJ onto the film's surface.

Results:

In the case of the binary compounds CdSe and CdS films, the diffraction spectra reveal a main peak at $2\theta = 25.4°$ and $2\theta = 25.35°$, respectively (Fig. 1), which are associated with the (002) crystalline plane of the hexagonal phase[7]. In addition, the ternary compounds' main peaks can be seen between these two peaks. As the temperature rises, the nuclei orientation tends to develop perpendicular arrangements along the substrate, allowing the atoms to gain enough energy for nucleation. This results in the hexagonal phase, which is often most noticeable in CdS (II-VI) films formed at high temperatures. The deposit's orientation along the *c*-axis perpendicular to the substrate is explained by the occurrence of the (002) peak, which is associated with the hexagonal structure[10].

According to Bragg's Law[11], the interplanar distance *d* was determined by utilizing the location of the primary peak in each diffractogram.

$$n = \frac{n\lambda}{2\sin\theta} \quad (1)$$

with λ = 1.54 Å the wavelength of *K*α copper emission, *n* any integer and θ the Bragg angle of reflection. According to previous report[12], the structural characteristics can also be connected to the interplanar distance *d*.

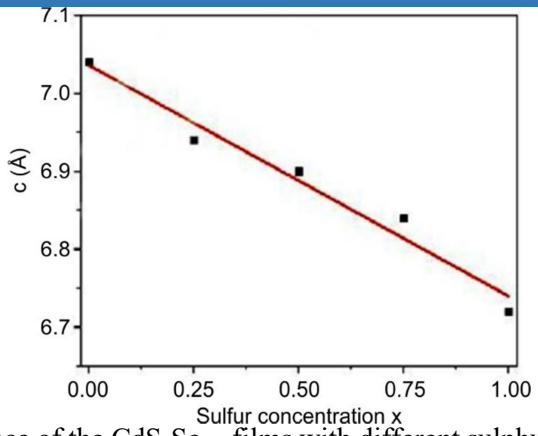

Fig. 2 Dependence of the CdS_xSe_{1-x} films with different sulphur concentration

UV-Vis spectroscopy: Transmittance spectra of all the CdS_xSe_{1-x} films, are shown in Fig. 3. It can be observed that there is a shift of the band edge from 550 nm, for CdS, to longer wavelength 790 nm, for CdSe, as a function of sulfur concentration. The transmittance spectra were analyzed in order to calculate the band gap energy for all the CdS_xSe_{1-x} samples. The calculation of the absorption coefficient (α) was performed by using the Essick method[16], according to the equation:

$$\alpha = -\frac{1}{d}\ln\left(\frac{\left\{(1-R)^4 + RT^2R^2\right\}^{1/2} - (1-R)^2}{2TR^2}\right) \quad (4)$$

where d is the optical thickness of the films; R is the reflection coefficient calculated in the transparent region of spectrum and T is the transmittance as a function of wavelength for the band edge. The energy band gap E_g can be obtained by extrapolating the linear regression of the plot $(\alpha h\nu)^2$ vs. $h\nu$ to zero[17], as it can be seen in Fig. 4, taking into account that the CdS_xSe_{1-x} semiconducting film have a direct band gap the energy values for all the samples are summarized in Table-2.

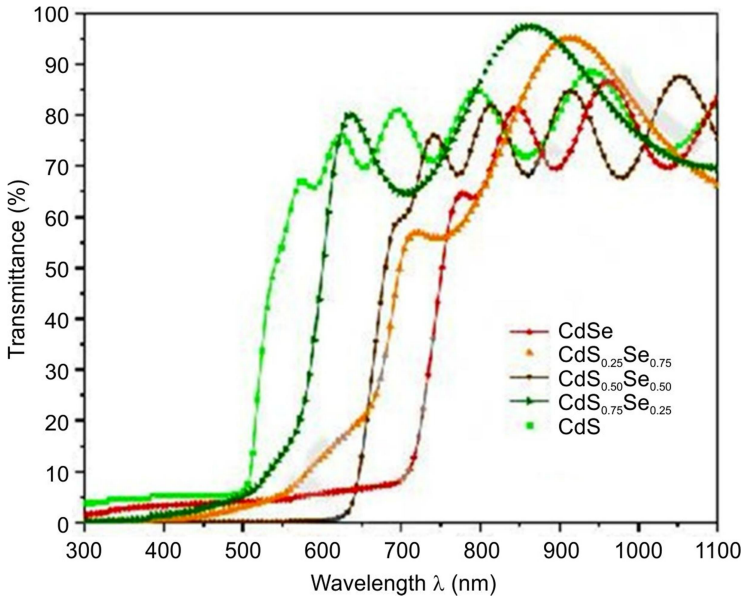

Fig. 3 UV spectra of the CdS_xSe_{1-x} films

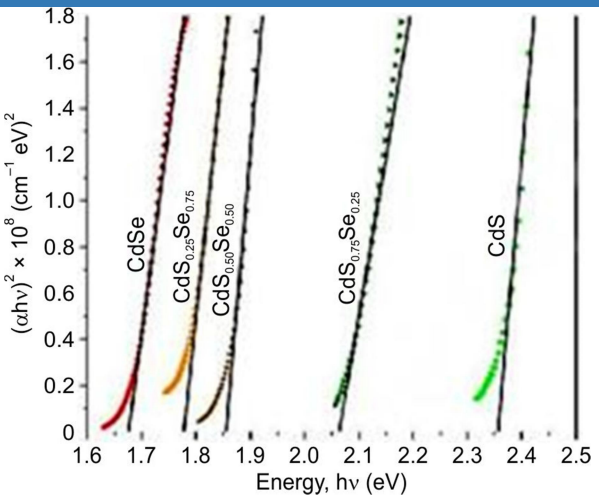

Fig. 4 Energy gap of the CdS_xSe_{1-x} films

The band gap values were used to visualize the dependence between the band gap energy E_g and the sulfur concentration x, which presents a non-linear behaviour which can be described earlier[7,18]

The experimental points fit the equation :

$$E_g(x) = 1.69 \cdot (1 — x) + 2.35 \cdot x — 0.62 \cdot x \cdot (1 — x) \quad (6)$$

The fitting parameters correspond to the energy band gap of CdS and CdSe, which agree whit values reported in literature[19,20]. The bowing parameter resulted be b = 0.62 eV, this has an upward bowing of the band gap, as commonly reported for CdS_xSe_{1-x}[18,21].

Photoluminescence spectroscopy: Based on the Photoluminescence (PL) measurements, Fig. 5 shows the normalized PL spectra at room temperature of the CdS_xSe_{1-x} films. As it can be seen a set of relatively narrow PL bands in the spectral range 1.5-2.6 eV are observed, each one for each CdS_xSe_{1-x} sample. The emission band at lowest energy, 1.70 eV, corresponds to CdSe, while the highest energy emission band, 2.41 eV, corresponds to CdS. It is possible to observe a shift to higher energy of the emission band by increasing the sulfur concentration. Usually, the energy of the emitted radiation is associated with transitions in the near band Edge (NBE), with the participation of donor–acceptors pairs (DAPs)[22]. The CdS film PL spectrum is the only one

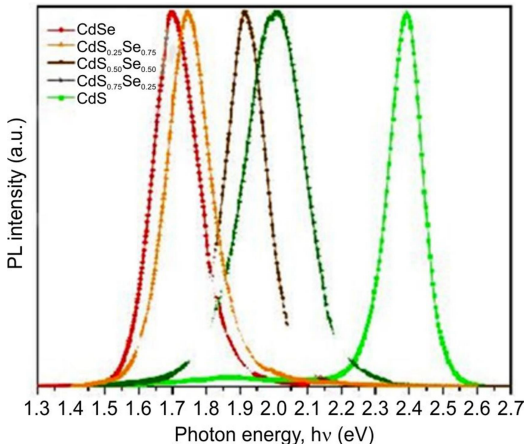

Fig. 5 PL spectra of the CdS_xSe_{1-x} films

which showed a second low intensity band located around to 1.8 eV, which according to the literature can be related to sulfur vacancies[23]. Furthermore, the symmetry and the width of the PL bands are related to good crystallinity on the films, as observed in the X-ray diffractograms. Because of the high deposition temperatures, the molecular species on the substrate surface gain more thermal energy, which increases the coalescence of the atoms giving rise to a film with uniform thickness and also a good crystallinity[24].

Raman spectroscopy: In order to analyze the structural properties of the CdS_xSe_{1-x} samples, they were analyzed by Raman spectroscopy, Fig. 6 shows the set Raman spectra, at room temperature. The spectra were recorded by using a He-Ne laser (633 nm) as excitation source. Usually CdS_xSe_{1-x} ternary compounds are classified within the so-called two mode behaviour alloys: CdS-like (LO) and CdSe-like (LO), *i.e.* characteristic of the binary compounds CdS and CdSe are simultaneously present for each intermediate concentration. These results suggest that scattering from the whole phonon is activated by disorder in CdS_xSe_{1-x} alloys[25]. In Fig. 7 it also can be seen two distinct phonon modes, the CdS-like LO mode (at 300 cm^{-1}) and the CdSe-like LO mode (at 206 cm^{-1}), which are associated with the hexagonal phase of each binary compound. CdS film have other signals, the first one at 210 cm^{-1} related to TO mode and the second one at 600 cm^{-1} related to 2LO mode. On the other hand the CdSe film have signal at 635 cm^{-1} related to 3LO mode. It can be also observed peaks at 293, 281, 277 cm^{-1} related to CdS in the ternary compounds as the concentration of sulfur decreases. In the same way, peaks at 198, 200, 204 cm^{-1} related to CdSe are present when changing the concentration of sulfur in the ternary alloys. The bands on the high energy side of Raman spectra are second-order modes, in the ternary films it can be observed the 2LO-CdS mode at 584 cm^{-1} for $CdS_{0.75}Se_{0.25}$, at 560 cm-1 for $CdS_{0.50}Se_{0.50}$, whereas the 2LO-CdSe mode can be seen at 415 cm^{-1} for CdS film and at 410 cm^{-1} for $CdS_{0.25}Se_{0.75}$ films. On the other hand, the overlapping of the LO-CdS + LO-CdSe phonon modes are present in the ternary compounds, at 490 cm^{-1} for $CdS_{0.75}Se_{0.25}$, at 483 cm^{-1} for $CdS_{0.50}Se_{0.50}$, and at 480 cm^{-1} for $CdS_{0.25}Se_{0.75}$[26,27].

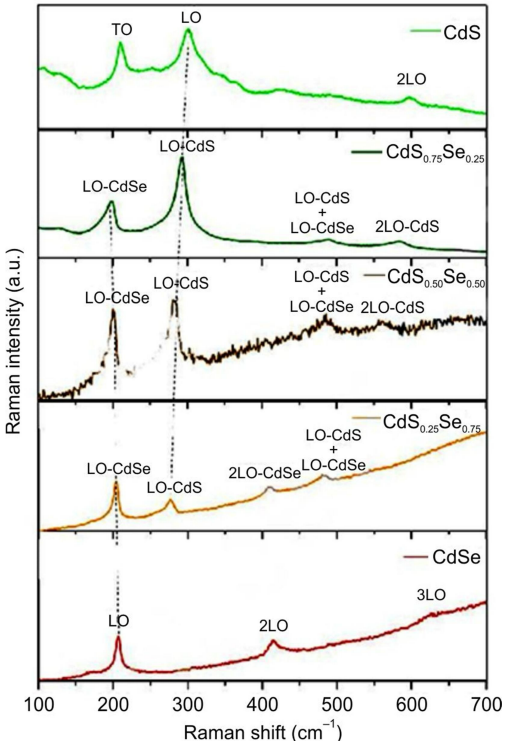

Fig. 6 Raman spectra of the CdS_xSe_{1-x} films

The contribution of the LO-CdS and LO-CdSe modes depends on the sulfur content. In fact, the decrease of sulfur concentration from de 0.75 to 0.25 yields a decrease of LO-CdS intensity as compared to the LO-CdSe mode. The asymmetry of the LO-CdS phonon peaks is attributed to phonon confinement or disorder effects, as the lattice disorder in the ternary compound mostly arises from the replacement of a heavier atom, selenium, for a lighter atom, sulfur[28]. It can be observed that the LO-CdS phonon mode frequency falls gradually as a function (decrease) of the sulfur content, which corresponds to an increase in selenium concentration, in good agreement with earlier reports[27]. This behaviour is a result of the ternary alloying effect, the Raman spectra (Fig 6) show that the phonon peaks are shifted and the dispersion intensity is smaller than the dispersion related to the binary compounds. Additionally, disorder also produces broadening of the Raman modes. Then, we shall assume that the band-edge LO phonon wavenumbers shift as the composition x changes in the same way as the corresponding Brillouin zone-center wavenumbers. In other words, the bending parameters of the dispersion curves vary linearly with x and vanish in the limit of $x \rightarrow 1$ for CdSe-like modes and $x \rightarrow 0$ for CdS-like ones. Because of the relatively large difference between the wavenumbers of the CdSe-like and CdS-like modes, they can be considered independently[29].

Conclusion:

At room temperature, films made of semiconductor ternary compounds with outstanding crystalline quality could be grown using the laser ablation technique. These compounds emit radiation in the visible range. Band gaps for deposited films ranged from 1.68 eV for CdSe to 2.39 eV for CdS, suggesting that different concentrations of sulfur could provide different band gaps. The Raman spectroscopy of the ternary samples, on the other hand, showed two phonons linked to LO-CdS and LO-CdSe, the strengths of which varied with the concentration of sulfur. It has been shown in nanocrystals and polycrystalline thin films that these Raman modes display non-symmetry, which may be associated with phonon confinement and disorder effects.

Conflict of Interest:

The authors declare that there are no conflicts of interest associated with this study.

Reference:

1. Pareek, A. & Borse, P. H. (2022) Hurdles and recent developments for CdS and chalcogenide-based electrode in “Solar electro catalytic” hydrogen generation: A review. *Electrochemical Science Advances*, *2*, e2100114.
2. Abbassi, A., Zarhri, Z., Azahaf, Ch., Ez-Zahraouy, H. & Benyoussef, A. (2015). Boltzmann equations and *ab initio* calculations: comparative study of cubic and wurtzite CdSe. *SpringerPlus*, 4(1), 543.
3. Bukhtiar, A. & Zou Bingsuo (2024). Low-dimensional II–VI semiconductor nanostructures of ternary alloys and transition metal ion doping: synthesis, optical properties and applications. *Materials Advances*, 5(17), 6739-6795.
4. Schröer, P., Krüger, P. and Pollmann, J., (1993). *Ab initio* calculations of the electronic structure of the wurtzite compounds CdS and CdSe. *Physics Reviews B*, 48, 18264.
5. Iqbal Khan, M. J. & Kanwal, Z. (2018). First principle calculations of optical properties of CdS:Al system (A DFT + U study). *Materials Research Express*, 6(3), 035905.
6. Soto-Montero, T. & Morales-Masis (2024), M. Laser Deposition of Metal Halide Perovskites, ACS Energy Letters, 9(8), 4199–4208.
7. Ahmed, N., Darwish, S. & Alahmari, A. M. (2011). Laser Ablation and Laser-Hybrid Ablation Processes: A Review. *Materials and Manufacturing Processes*, 31(9), 1121-1142.
8. Šedo, O., Alberti, M. & Havel, J. (2005). J. Laser ablation synthesis of new binary chalcogen molecules from the selenium–sulfur system, Polyhedron, 24(5), 639-644.

9. Haider, A. J., Alawsi T., Haider, M. J. & Taha, B. A. & Marhoon, A. A. (2022). A comprehensive review on pulsed laser deposition technique to efective nanostructure production: trends and challenges. Optical and Quantum Electronics. 54, 488.

10. Sudjatmoko S., Wirjoadi W. & Siswanto, B. (2019). Influence of Substrate Temperature on Structural, Electrical and Optical Properties of ZnO:Al Thin Films. Atom Indonesia, 35(2), 115-125.

11. Liu, Y., Yu, H., Drew, M.G.B. & Liu, Y. (2018) A systemized parameter set applicable to microwave absorption for ferrite based materials. Journal of Materials Science: Materials in Electronics, 29(2), 1562–1575.

12. Liu, Y., Liu, Y. & Drew, M.G.B. (2020). Clarifications of concepts concerning interplanar spacing in crystals with reference to recent publications. SN Applied Sciences, 2, 755.

13. Hargreaves, J. S. J. (2016). Some considerations related to the use of the Scherrer equation in powder X-ray diffraction as applied to heterogeneous catalysts. Catalysis, Structure & Reactivity, 2(1–4), 33–37.

14. A. R. Denton & N. W. Ashcroft (1991), Vegard's Law, Physics Reviews A, 43, 3161.

15. Aresti, A., Congiu, A., Manca, P., & Spiga, A. (1973). Thermal conductivity of CdS_xSe_{1-x} solid solutions. Journal of Applied Physics, 44(8), 3401-3403.

16. Essick, J. M. & Mather, R. T. (1993). Characterization of a bulk semiconductor's band gap via a near-absorption edge optical transmission experiment. American Journal of Physics, 61(7), 646–649.

17. Tauc, J., Grigorovici, R. & Vancu, A. (1966). Optical properties and electronic structure of amorphous germanium, Physica Status Solidi, 15, 627–637.

18. Hill, R. (1974). Energy-gap variations in semiconductor alloys. Journal of Physics C: Solid State Physics, 7(3), 521.

19. Karim, M. R., Balaban, M. & Ünlü, H. (2019). Strain Effects on the Band Gap and Diameter of CdSe Core and CdSe/ZnS Core/Shell Quantum Dots at Any Temperature, Advances in Materials Science and Engineering, 3764395, 1-10.

20. Wang, X., Yu, J. & Chen, R. (2018). Optical Characteristics of ZnS Passivated CdSe/CdS Quantum Dots for High Photostability and Lasing. Scientific Report, 8, 17323.

21. Khan, I., Ahmad, I., Aliabad, H. R., Asadabadi, S. J., Ali, Z., & Maqbool, M. (2013). Conversion of optically isotropic to anisotropic CdS_xSe_{1-x} ($0 \leqslant x \leqslant 1$) alloy with S concentration. Computational Materials Science, 77, 145-152.

22. Ullrich, B., Bagnall, D. M., Sakai, H., & Segawa, Y. (2000). Photoluminescence and lasing of thin CdS films on glass formed by pulsed-laser-deposition. Journal of Luminescence, 87, 1162-1164.

23. 23. Aguilar-Hernandez, J., Sastre-Hernandez, J., Mendoza-Perez, R., Contreras-Puente, G., Cardenas-Garcia, M., & Ortiz-Lopez, J. (2006). Photoluminescence studies of CdS thin films annealed in $CdCl_2$ atmosphere. Solar Energy Materials and Solar Cells, 90(6), 704-712.

24. Rafea, M. A., Farag, A. A. M., & Roushdy, N. (2009). Structural and optical characteristics of nano-sized structure of $Zn_{0.5}Cd_{0.5}S$ thin films prepared by dip-coating method. Journal of Alloys and Compounds, 485(1-2), 660-666.

25. Pagliara, S., Sangaletti, L., Depero, L.E., Capozzi, V., Perna, G. (2000). Effect of disorder on the Raman scattering of CdS_xSe_{1-x} films deposited by laser ablation. *Solid State Communications*, 116, 115–119.

26. Díaz-Reyes, J., Contreras-Rascón, J.I., Arias-Cerón, J.S., Sánchez-Ramírez, J.F., GalvánArellano, M., Martínez-Juárez, J., Balderas-López, J.A. (2015). Structural and optical characterization of $CdSe_{1-y}S_y$. *Materials Science in Semiconductor Processing*, 37, 199–206.

27. Dzhagan, V. M., Azhniuk Y. M., Milekhin, A. G., Zahn, D. R. T. (2018). Vibrational spectroscopy of compound semiconductor nanocrystals. *Journal of Physics D: Applied Physics*, 51, 503001.

28. Alcalde, A.M., Ribeiro, A.A., Dantes, N.O., Mendes Jr., D.R., Marques, G.E., Trallero-Giner, C. (2006). Optical phonons and Raman scattering in ternary II-VI spheroidal nanocrystals embedded in a glass matrix. *Journal Non-Crystal Solids*, 352, 3618e3623.

29. Freitas Neto, E., da Silva, S. W., Morais, P. C., Vasilevskiy, M. I., Pereira-da-Silva, M. A., Dantasa, N. O. (2011). Resonant Raman scattering in CdS_xSe_{1-x} nanocrystals: effects of phonon confinement, composition, and elastic strain. Journal of Raman Spectroscopy, 42, 1660–1669.